JOURNAL OF GEOPHYSICAL RESEARCH, VOL. 104, NO. A1, PAGES 355-370, JANUARY 1, 1999

Earthward flow bursts in the inner magnetotail and their relation to auroral brightenings, AKR intensifications, geosynchronous particle injections and magnetic activity

D. H. Fairfield,[1] T. Mukai,[2] M. Brittnacher,[3] G. D. Reeves,[4] S. Kokubun,[5] G. K. Parks,[3] T. Nagai,[6] H. Matsumoto,[7] K. Hashimoto,[7] D. A. Gurnett,[8] T. Yamamoto[2,9]

Abstract. High-velocity magnetotail flow bursts measured by the Geotail Low Energy Plasma experiment in the premidnight equatorial region between 10 and 15 R_E have been compared with other magnetospheric phenomena. These bursts, typically characterized by earthward velocities approaching 1000 km/s and lasting for times of the order of 1 min, are associated with magnetotail dipolarizations and large magnetic field fluctuations. Using supporting measurements of the International Solar Terrestrial Physics program it is found that the flow bursts are closely associated with auroral brightenings, AKR onsets, geosynchronous particle injections, and ground magnetic activity. Flow bursts for which Polar UVI images are available showed auroral brightenings that developed near the footpoint Geotail field line. AKR intensifications usually accompanied the flow bursts in close time coincidence, whereas dispersionless geosynchronous particle injections tended to be delayed by 1–3 min. Since flow bursts often exhibit the earliest onsets of these various phenomena, it seems likely that this chain of events is initiated in the tail beyond 15 R_E, presumably by magnetic reconnection. It is concluded that flow bursts are a fundamental magnetotail process of limited spacial extent that are important in energy and magnetic flux transport in the magnetosphere. Magnetotail flow bursts are intimately connected to auroral acceleration processes and AKR generation at several thousand kilometer altitude and a full explanation of substorms will have to explain this relationship.

1. Introduction

A major advance in substorm research over the past decade has been the realization that magnetotail convection takes place largely in the form of discrete bursts of high-velocity flow of limited spatial extent [e.g., *Angelopoulous et al.*, 1996, and references therein; *Shiokawa et al.*, 1997, 1998; *Fairfield et al.*, 1998; *Petrukovich et al.*, 1998]. These flows can achieve velocities up to 2000 km/s [*Fairfield et al.*, 1998] for times of the order of a minute, with such short "flow bursts" [*Angelopoulous et al.*, 1992] or "impulsive dissipation events" [*Sergeev*, 1996] tending to be grouped within intervals of 5 to 10 min termed "bursty bulk flows" [*Angelopoulos et al.*, 1992]. *Sergeev et al.* [1996] propose that these short bursts in the magnetotail constitute the smallest fundamental process that makes up substorms. It is known that earthward flow bursts are associated with increases in tail magnetic field B_z (i.e., dipolarizations) and substorm expansion phase onsets [e.g., *Angelopoulous et al.*, 1996], although they can also occur when the equatorial magnetic field in the tail is already quite northward and geomagnetic conditions are quiet [*Angelopoulos et al.*, 1992].

In a similar manner, improved time and spacial resolution of auroral images has revealed that auroral brightenings often occur in limited spatial regions and at times other than during full-fledged substorm onsets. Small precursory brightenings often occur before the onset [e.g., *Elphinstone et al.*, 1995b], and they are not necessarily restricted to the region of the subsequent onset [*Murphree et al.*, 1991]. When the substorm is initiated, there is first an "initial brightening" [e.g., *Kaneda and Yamamoto*, 1991] in a region often limited to less than 1 hour of local time. This brightening is followed within a few minutes by a "flaring up" [*Kaneda and Yamamoto*, 1991] as the region expands. *Rostoker* [1998] proposes that small scale auroral brightenings (surges) and their associated magnetosphere/ionosphere currents (wedgelets) form the smallest fundamental process at low altitudes.

Studies comparing auroral kilometric radiation (AKR) and the geomagnetic AE index have revealed a close association of AKR and geomagnetic substorms [*Gurnett*, 1974; *Voots et al.*, 1977; *Kaiser and Alexander*, 1977], but since the AE index is not a precise indicator of substorm onset times, the exact time relation of substorm onsets to AKR is not known. Kaiser and Alexander

[1] Laboratory for Extraterrestrial Physics, NASA Goddard Space Flight Center, Greenbelt, Maryland.

[2] ISAS, Sagamihara, Japan.

[3] Geophysics Program, University of Washington, Seattle, Washington.

[4] Los Alamos National Laboratory Los Alamos, New Mexico.

[5] STELAB, Nagoya University, Nagoya, Japan.

[6] Earth and Planetary Sciences, Tokyo Institute of Technology, Tokyo, Japan.

[7] Radio Atmospheric Science Center, Kyoto University, Uji, Kyoto 611, Japan.

[8] University of Iowa, Iowa City, Iowa.

[9] Deceased February 1998.

Paper number 98JA02661.
0148-0227/99/98JA-02661$09.00

found that typically AKR begins at the higher frequencies during the substorm growth phase and then intensifies and expands in bandwidth (particularly to lower frequencies) near the time of onset. This early study, however, could not employ modern means of determining substorm onsets.

Flow bursts are seen most frequently beyond 15 R_E [*Shiokawa et al.*, 1997] and are generally supposed to be distinct from "current disruption events" seen by the AMPTE/CCE spacecraft inside of 9 R_E [e.g., *Lui*, 1996]. The magnetic signatures of both classes of events are similar, however, and since (1) the primary thermal ion experiment on CCE had failed by the time CCE entered the tail and measured the disruptions and (2) the energetic particle experiment on CCE looked perpendicular to the spin axis which pointed toward the sun (and hence also toward the Earth in the relevant midnight region), it is unlikely this spacecraft would have seen any earthward flows associated with the disruptions. It should be noted that such flows when seen near the equator do not necessarily follow field lines and hence seeing maximum fluxes at the smallest pitch angles [*Lopez et al.*, 1989] is not necessarily a measure of particle flows. Bursts of high velocity flow in the ionosphere have also been seen by the ground radars [*Williams et al.*, 1992; *Lewis et al.*, 1998].

In the study reported below, we will investigate the extent to which flow bursts in the magnetotail correspond to the remote detection of AKR intensifications and also auroral brightenings and their associated magnetosphere/ionosphere currents. We find a good time correspondence among these phenomena, suggesting that they are all basic elements which, under appropriate circumstances, may form a magnetospheric substorm.

2. Observations

A common procedure for studying magnetospheric substorms is to first identify events using data taken on the ground or in geosynchronous orbit and then collect supporting information from as many additional spacecraft as possible. If magnetotail fast flows are of very limited spatial extent, however, a magnetotail spacecraft will seldom be in the appropriate place to detect these flows. Therefore it makes more sense to first look for the fast flows and then determine if or how they relate to geomagnetic activity and accompanying processes. This is the approach taken in the present paper.

To investigate the equatorial region between 10 and 15 R_E often not well covered by earlier spacecraft, we have scanned the Geotail data in May 1996 when the spacecraft spends time near the equatorial current sheet in this distance range. Magnetic field dipolarizations associated with high-frequency fluctuations (as revealed by enhanced root mean square standard deviations over 3 s intervals) are frequently found to be associated with fast magnetotail flows that can be identified in key parameter data or in on-line spectograms of the Geotail Low Energy Plasma (LEP) experiment. Dipolarization events are more common than high-flow events because dipolarizations can be detected away from the equatorial plane and/or they are sometimes more gradual and not associated with rapid field fluctuations. High time resolution Geotail plasma moment data (12 s resolution) and supporting ground and spacecraft data were then obtained for the several events described below. Figure 1 illustrates the locations of several events that will be discussed below. Note that the events are in the premidnight region where substorm flows have been shown to concentrate at greater distances [*Nagai et al.*, 1998].

2.1. May 4, 1996, Small Substorms

On May 4, 1996, Geotail was located near Xsm=-13., Ysm=3.5 R_E (2300 LT) when it observed two flow bursts at 0555 and 0627 UT with velocities reaching 800 km/s. These flows can be seen in Figure 2d. The Geotail magnetic field magnitude and solar

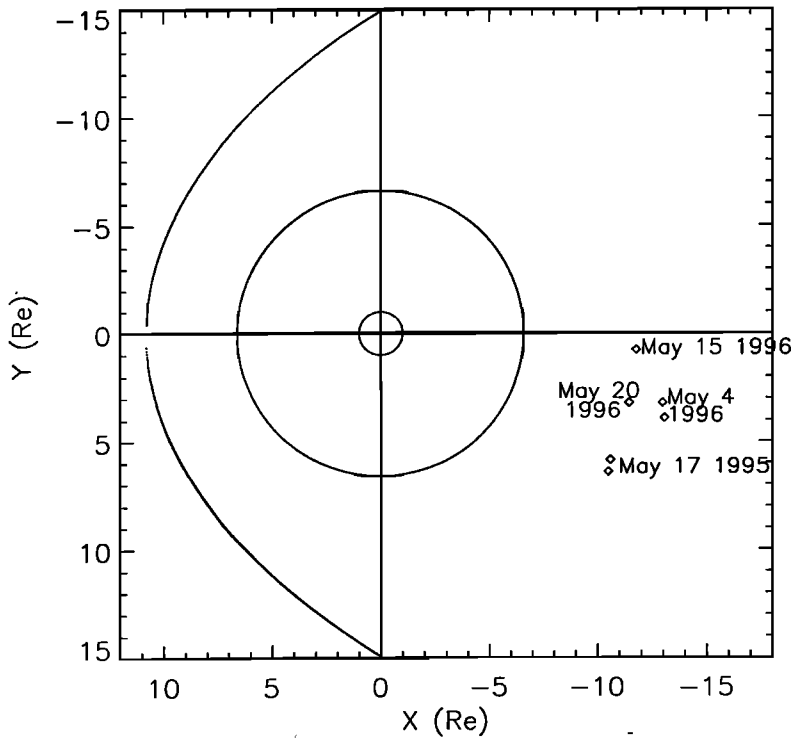

Figure 1. Symbols indicate the location of the equatorial flow bursts used in this study. The Sun is toward the left, and solid lines represent the magnetopause and the geosynchronous orbit.

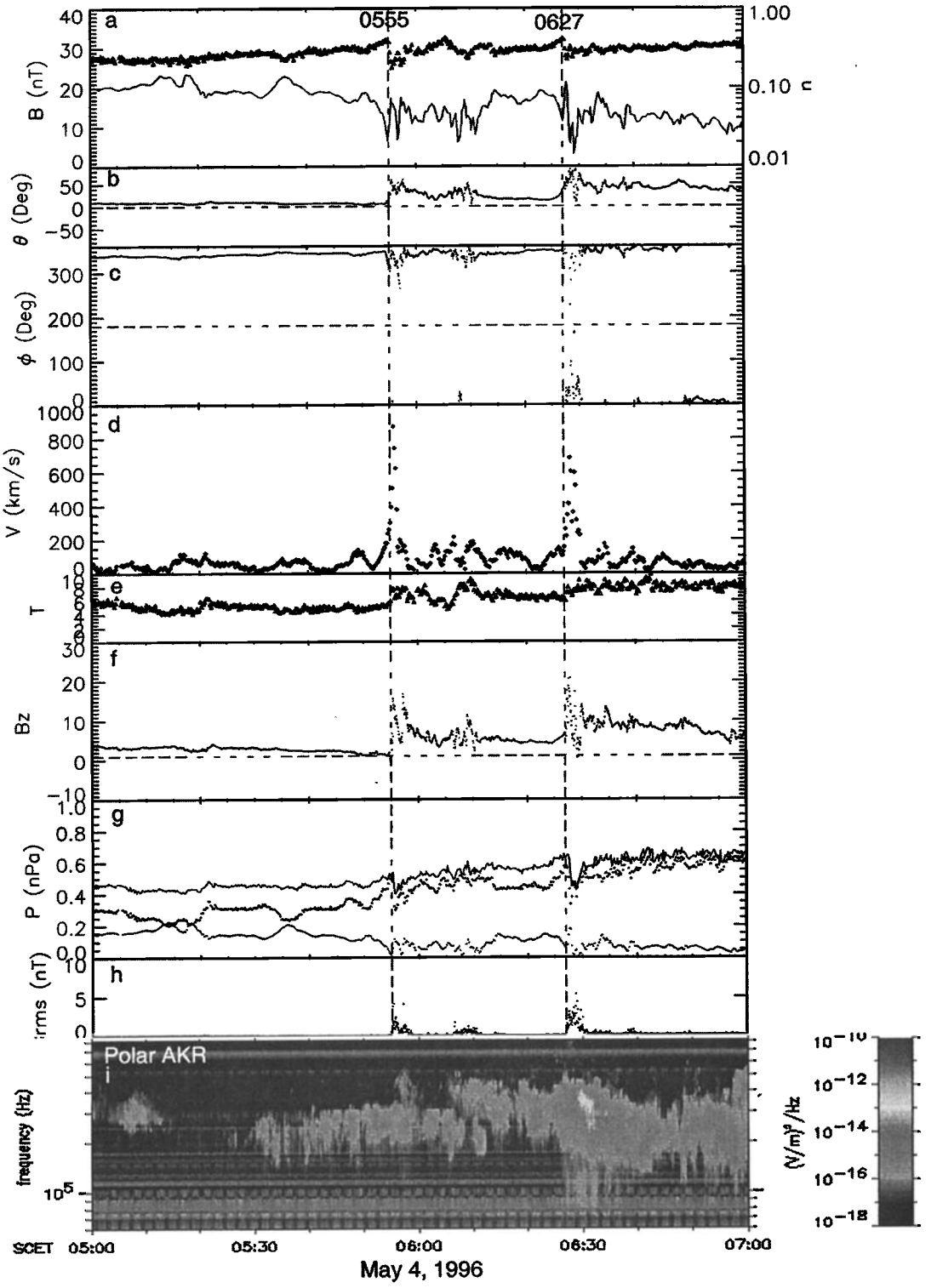

Figure 2. Two high-velocity flow bursts observed by Geotail near the equator at 14 R_E and 2300 LT during very a moderate (150 nT) disturbance: (a) Geotail magnetic field and density with lines and heavy symbols, respectively; (b) and (c) the magnetic field latitude and longitude angles; (d) velocity; (e) ion temperature; (f) B_z component of the magnetic field; (g) magnetic field pressure (bottom solid line), the plasma pressure (heavy symbols), and sum of the two. (h) root mean square deviation of the magnetic field associated with the 48 vector measurements constituting each 3 s vector average; (i) electric field wave intensity measured by the plasma wave instrument on the Polar spacecraft in the AKR frequency range (hundreds of kilohertz). The flow bursts at times marked with vertical dashed lines are accompanied by magnetic field dipolarizations in the typical manner. AKR intensifies near the onset of each burst.

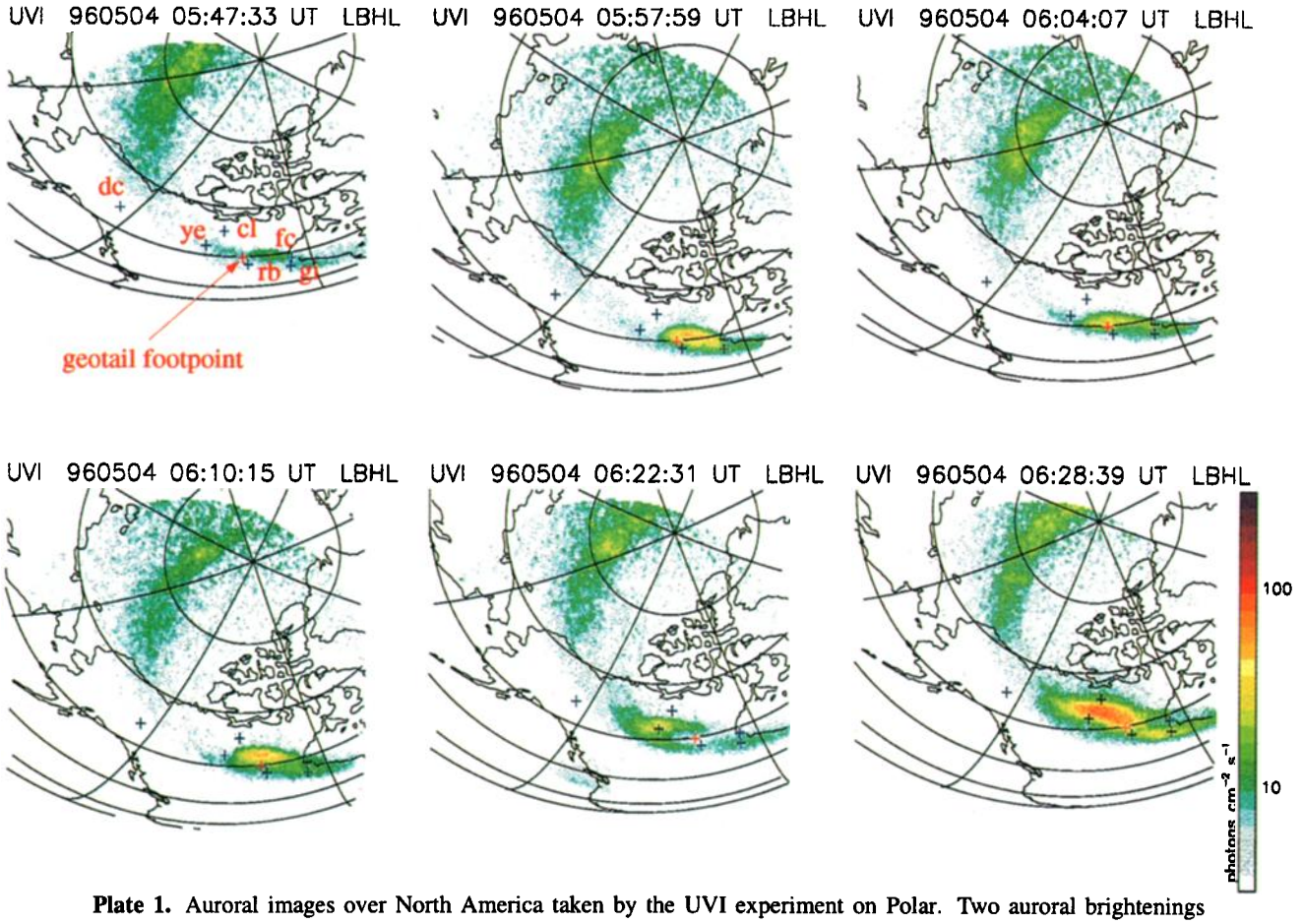

Plate 1. Auroral images over North America taken by the UVI experiment on Polar. Two auroral brightenings develop very close to the Geotail footpoint between the 0547:33 and 0557:59 UT images and between the 0622:31 and 0628:39 UT image. These times are in close correspondence to the 0555 and 0627:15 UT flow burst onsets.

magnetospheric latitude and longitude angles are displayed in the Figure 2a-c. Density is also displayed with heavy symbols in Figure 2a. Subsequent panels include proton temperature T in keV (Figure 2e), the B_z component of the magnetic field (Figure 2f), the total pressure (top trace in Figure 2g) as the sum of the thermal pressure (indicated by heavier symbols) and the magnetic pressure, the root-mean-square error of each 3 s magnetic field average (Figure 2h), and the Polar electric field wave intensity in the AKR frequency range (Figure 2i). The abrupt increase in B_z and theta angle that typically accompanies flow bursts is clearly seen. Geotail was estimated to be only 0.1 R_E above the equatorial current sheet [*Fairfield*, 1980], which is consistent with the high ratio of plasma to magnetic field pressure and the fact that Geotail crossed the current sheet 90 min later. Although AKR did not intensify at the time of the flow burst as dramatically as in some events, it extended to higher frequencies at 0555 and intensified at about 0627.

An expansion of the interval 0625–0635 on May 4 is shown in figure 3. Parameters similar to figure 2 are plotted except that the magnetic field is displayed here at its highest resolution (16 measurements/s) and triangles indicate the density and flow directions in Figures 3a-3c.. Figure 3d also displays flow vectors in the XY plane which represent only flow perpendicular to the magnetic field. Flow toward the Sun is upward, and flow toward dusk is to the left. Figure 3e shows both total and perpendicular flow vectors with large and small symbols respectively. The high-frequency variations in the magnetic field seen during the high flows are characteristic of flow bursts as well as "current disruption events" seen by AMPTE CCE near 8 R_E.

Auroral observations from the UVI experiment in the LBHL band [*Torr et al.*, 1995] were available for this event and selected images from the interval 0547–0628 are shown in Plate 1. The locations of selected Canadian ground stations are shown in the quiet image at 0547:33 UT where the auroral oval can barely be discerned. (Note that all image times in this paper are the begin times of 36 s integration intervals.) The location of the Geotail footpoint is indicated with a red plus sign that is very close to Rabbit Lake (rb). (All mapping in this paper were done with the T87 model [*Tsyganenko*, 1987] using level 4 thought to be appropriate for pre-onset conditions. Mappings with the T96 model [*Tsyganenko*, 1995, 1996] were carried out and tended to differ by about a degree of latitude and a few degrees longitude, but this model is not easily adjusted to more stretched conditions and therefore was not used.) The 0557:59 UT image taken 3 min after the first flow burst shows a brightened aurora very near the location of the mapped Geotail field line. The brightened aurora is also apparent in the 1304 image at 0555:32 (not shown) which even more strongly supports the association of the brightening and the 0555 flow burst. The aurora fade in the 0604:07 UT image in Plate 1 and brighten slightly in the image at 0610:15 UT which closely follows a small disturbance/dipolarization that can be seen in figure 2. The aurora fade again and then brighten

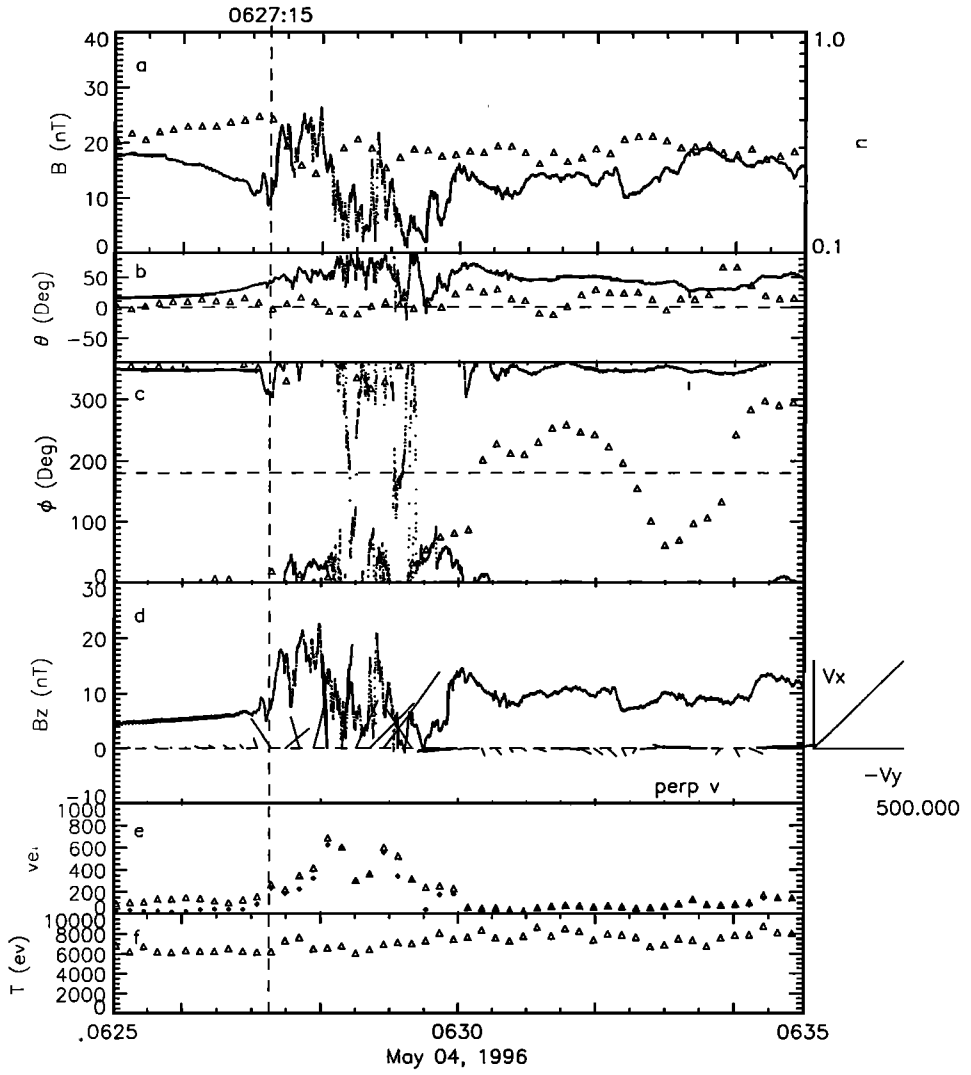

Figure 3. Ten minutes of data during the second flow burst shown in Figure 2. Parameters are basically the same as in Figure 2 except the magnetic field is shown at its highest resolution of 16 measurements/s. Flow velocity direction is indicated by the triangles in (b) and (c). Vectors in (d) show the equatorial flow velocity perpendicular to the field with the sunward direction up and the duskward direction to the left. The large and small symbols in the velocity panel indicate the total and perpendicular velocity. High-frequency magnetic field fluctuations invariably accompany high velocities.

more dramatically between the 0622:31 and 0628:39 UT images that span the time of the 0627 UT flow burst. Brightening occurs between LBHS images at 0623:44 and 0628:11 UT (not shown) which further restrict the onset to this interval and hence strengthens the correspondence to the 0627 UT flow burst.

The comprehensive network of Canadian magnetic observatories supports the impression that these are events of limited intensity as well as small area. Only a very small perturbation at Rabbit Lake (rb) slightly south of the brightening was associated with the 0555 UT burst and a 150 nT negative bay at Contwoyto Lake (cl) and Fort Churchill (fc) was associated with the 0627 UT burst. Note that this 0627 UT brightening occurred west of the 0555 UT brightening and was beginning to develop in the 0622:31 UT image in Plate 1; indeed a small magnetic perturbation at Yellowknife (ye, not shown) which was almost coincident with the brightening, was beginning to develop as early as 0617 UT. This fact suggest that some communication between the ionosphere and magnetosphere begins prior to the time of major brightening that would normally be judged expansion phase onset. Note also that the maximum perturbations are near the poleward boarder of the aurora where the initial substorm currents tend to be strongest [*Pulkkinen et al.*, 1998, and references therein].

There was no clear particle injection signature for these events at the Los Alamos geosynchronous spacecraft, the most strategically placed of which was located about 4 hours after midnight. The GOES 9 spacecraft at 2130 LT saw no effect at 0555 UT but it did see an initial decrease at 0627 UT with an increase 4 min later which is characteristic of a geosynchronous spacecraft west of a current wedge. GOES 8 at 0130 LT and ETS-VI near 1900 LT saw no effects.

These two flow bursts on May 4 show how large flows of the order of 800 km/s accompany even modest auroral brightenings and weak AKR intensifications. The bursts were seen very near the equatorial location of the mapped, brightened region, and it

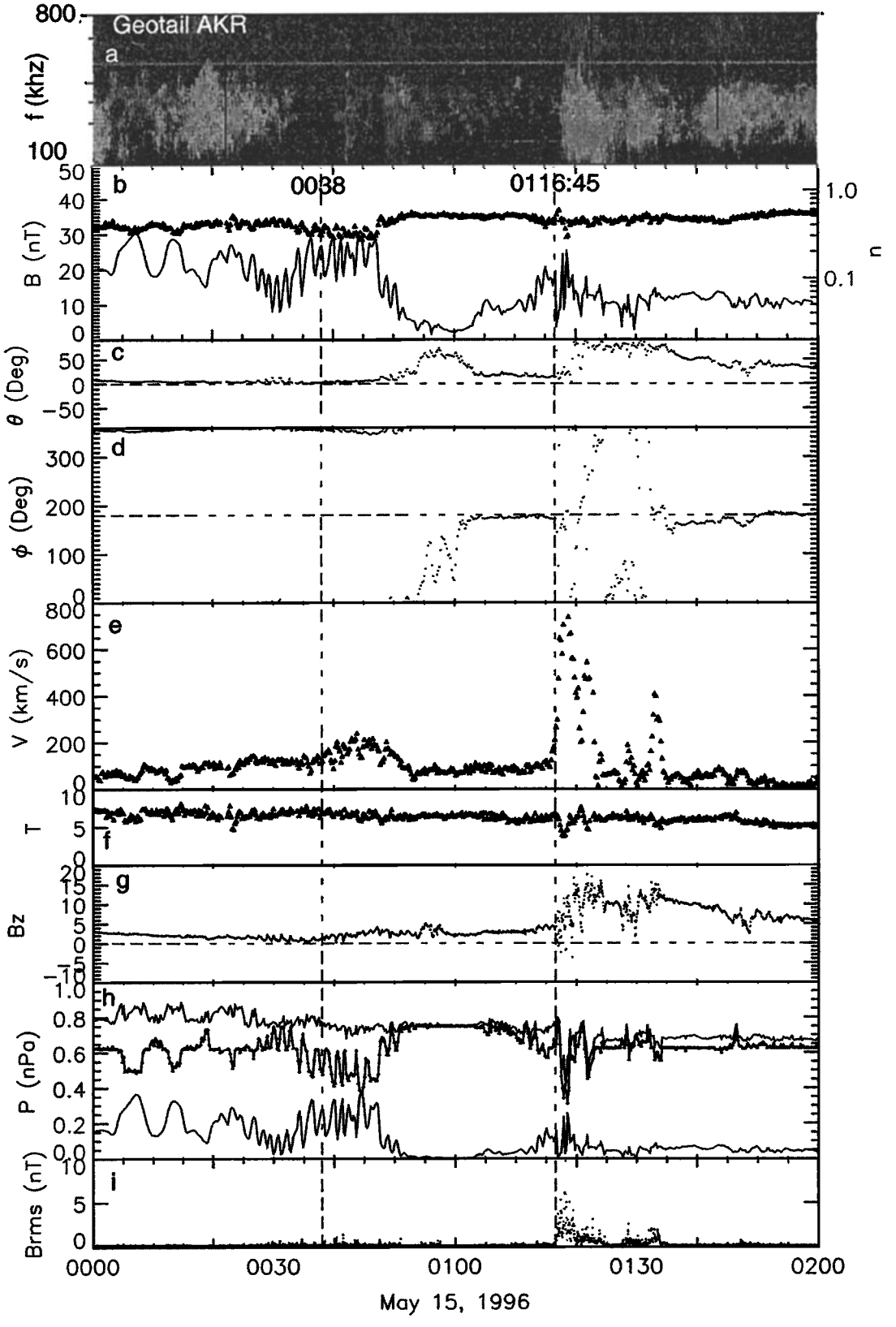

Figure 4. In a format equivalent to Figure 2, a flow burst is seen near local midnight at 12 R_E at 0116:45 UT in close coincidence with a Geotail AKR intensification. A geosynchronous spacecraft observed a dispersionless onset at the earlier time of 0038 UT when Geotail saw a small B_z increase and weak flow, but any large flow burst associated with this event was probably too far from Geotail to be seen. Geosynchronous data terminated before 0116 UT.

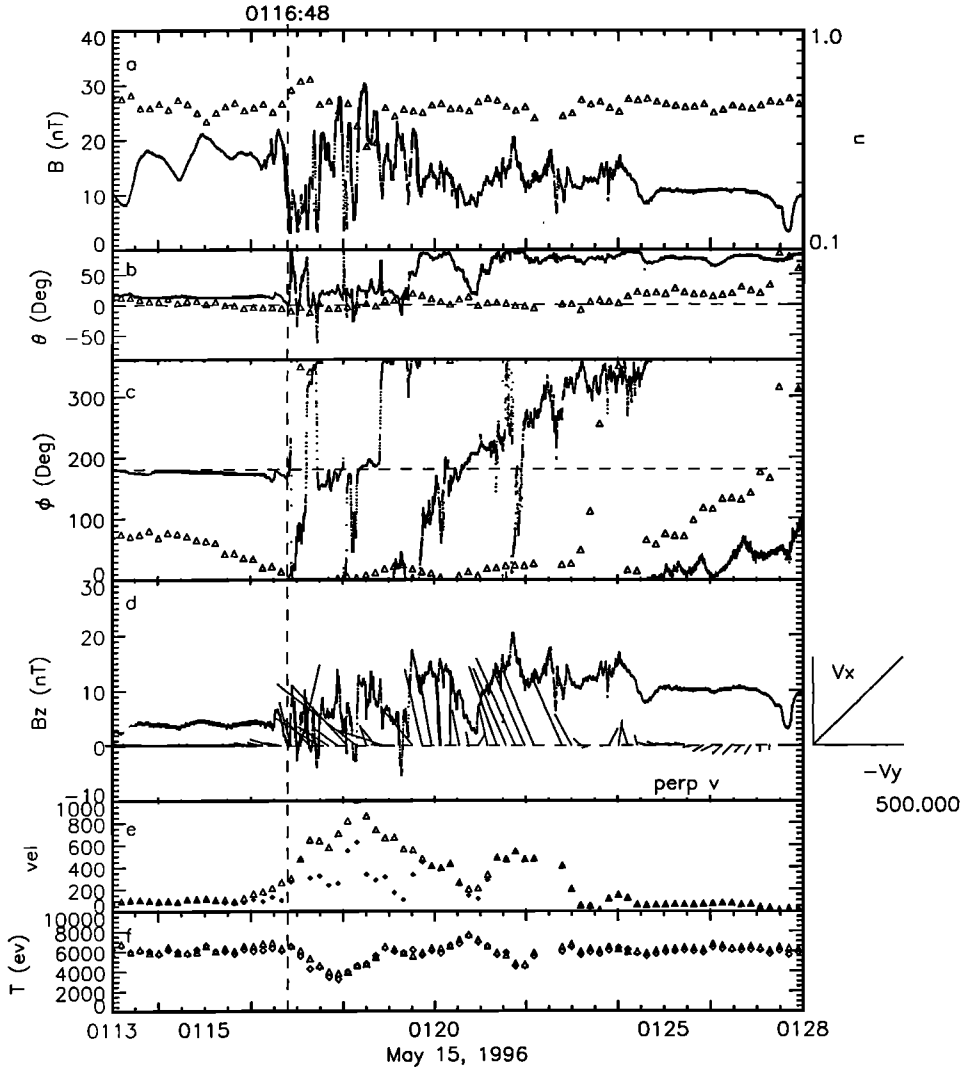

Figure 5. High-resolution data for the 0116 UT flow burst of Figure 4 in the format of Figure 2. Geotail was extremely close to the equatorial plane as evidenced by the ϕ reversals between 0116 and 0119 UT.

seems unlikely the bursts would have been seen elsewhere in the magnetotail.

2.2. May 15, 1996, Substorm

Figure 4 shows 2 hours of data on May 15, 1996, when Geotail was located at Xsm=-11.8, Ysm=0.8 R_E (2345 LT). The format is essentially the same format as Figure 2 except Geotail AKR data are shown in Figure 4a. Geotail observed a large flow burst and B_z increase beginning at 0116:45 UT, only 15 min after it had slowly passed through a very quiet equatorial current sheet. Geotail remained in a high-beta plasma throughout the interval as can be seen by the dominance of plasma pressure over magnetic pressure in Figure 4h. The polar spacecraft was near perigee with no images or AKR data available, but the plasma wave instrument on Geotail detected a clear AKR onset at 0117 UT (Figure 4a).

Higher resolution data are shown in Figure 5 in the same format as Figure. 3. It is clear from the ϕ angle reversals between 0117 and 0119:30 UT that Geotail is very near a thinned, oscillating current sheet during the large flow interval. The θ angle did not increase until 2.5 min after the start of the flow burst which may be when a tailward moving region of accumulating northward flux moved over the spacecraft. During this 2.5–min interval about half the flow is field aligned (Figure 5e) and the perpendicular component is earthward and duskward (Figure 5d). After this interval when the field becomes almost entirely northward, a field of 12 nT is being carried earthward at a velocity near 500 km/s. It should also be noted that in the minute between 0116 and 0117 UT while the magnetic field was still quiet, the velocity measured by Geotail in this equatorial location increased from about 50 to 300 km/s before the more dramatic increase to 800 km/s began. This early velocity increase is largely in the parallel component, and it appears to precede the AKR onset, providing support for the view that events in the tail occur before other phenomena.

On this day, geosynchronous spacecraft did not collect data in positions where they would be expected to observe this event. A geosynchronous spacecraft did detect a dispersionless onset at the earlier time of 0038 UT and 2200 LT (not shown), but data collection at this spacecraft terminated before 0117 UT. This 0038 UT time corresponded to the start of a slow B_z increase and modest duskward flow at Geotail (Figure 4g and 4e) which was probably too far to the east to see any large flow and sharp

dipolarization. No substorms were apparent in the Image chain of magnetometer data in the postmidnight region, but coverage was not good at earlier local times.

Note that *Pulkkinen et al.* [1998] studied two prominent substorms 6 hours later on this day, but Geotail in the plasma sheet at a location near 0300 LT showed only a delayed magnetic field reconfiguration at this later local time and it detected no flows exceeding about 200 km/s.

2.3. May 14, 1996, Substorm

An interval on May 14, 1996, included good Polar images, AKR data, and geosynchronous particles. Aurora brightened in a 1749:35 UT image (not shown) just east of the mapped Geotail field line near 1900 LT. This brightening is apparently associated with a Geotail B_z increase marked by a vertical dashed line at 1748 UT in Plate 2, which was detected as this spacecraft resided in a strong lobelike field. Stations of the Image magnetometer chain in the region of the brightening also saw a modest negative perturbation beginning at 1748 UT. Only after this time did Geotail make excursions into the weaker-field plasma sheet where it saw a hotter, earthward flowing plasma (not shown).

Aurora in the slightly premidnight region gradually faded (see the 1757:06 UT panel in Plate 3) until a brightening occurred after the 1759:06 UT image (not shown). This brightening was just beginning in the 1759:34 UT image in Plate 3 and was much intensified in the 1802:01 UT image. The brightening covered the region of the footpoint of the Los Alamos 1991–080 spacecraft at 2240 LT and indeed this spacecraft saw a dispersionless injection of electrons and protons at 1800:56±4s UT (Plates 2d and 2e). Polar measurements of AKR in Plate 2g revealed an initial increase at 1759:50 UT near 100 kHz, an intensification at 1800:30 UT near 60 kHz, and a further large intensification at 1801 UT. Geotail saw no effects of this intensification/injection near 1800 UT since the event was located about 2 hours east of Geotail.

After this 1800 event the bright aurora covering a broad range of longitude moved northward over the next 30 min as indicated by the last three images in Plate 3. Geotail made several excursions into the plasma sheet/boundary layer and finally remained immersed in the plasma sheet after about 1816 UT, which is about the time the northward moving auroral expanded over the spacecraft footpoint. Ground magnetic perturbations increased in a region of brightening aurora between 1814:17 and 1816:44 UT but large flows at Geotail at 1814 UT (not shown) were mostly field aligned because the spacecraft was not so near the center of the current sheet. Geotail also observed a increase in B_z but not the highly variable fields that are characteristic of the equatorial region. The sharp increase in Geotail field latitude at 1816 UT was not accompanied by particularly large flows and was due largely to the spacecraft passing into the plasma sheet which caused a decrease in B_x, but not an abrupt increase in B_z.

This interval of data demonstrates the localization of auroral brightenings and importance of local time in interpreting spacecraft data. Geotail saw a B_z increase associated with the small 1748 UT intensification not too far from its location even though it was in the lobe. On the other hand, Geotail was at too early a local time to see the larger onset 2 hours to the east at 1800 UT. A geosynchronous spacecraft at the proper local time did see a dispersionless onset at this time, although it was delayed slightly relative to the AKR onset. Such delays are consistent with the idea that flow bursts are the cause of injections.

2.4. May 20, 1996, Substorms

At 0030 UT on May 20, 1996, Geotail was located at 16.6 R_E in the tail lobe just past 2000 LT (Xsm=-9.2, Ysm=12.7, Zsm=5.4 R_E). IMP 8 was also in the tail lobe at 2300 LT and 17 R_E further down the tail (Xsm=-26.0,Ysm=6.4, Zsm=-11.9), thus providing an opportunity to investigate lobe field changes relative to AKR and aurora. Magnetic field, plasma, and AKR data are shown in Plate 4. AKR exhibited a small intensification at 0025 UT followed by a stronger intensification at 0029:30 UT. This latter time followed the beginning of a lobe field decrease at Geotail by one min. An IMP 8 decrease followed Geotail by 5 min which gives a downtail propagation velocity of $17R_E/5$ min = 360 km/s. Gradual B_z increases at these two spacecraft were delayed by a minute or two relative to their respective B decreases.

Energetic electron fluxes from the Los Alamos geosynchronous spacecraft 1990–095 are shown in Figure 6 along with the Geotail magnetic field. These electron fluxes measured near 2200 LT show an initial dispersionless increase at 0030 UT and a larger dispersionless increase at 0033 30s UT. This timing suggests that these two increases may be related to the earlier weak Polar AKR onset at 0025:30 UT and the stronger onset at 0029:30 UT. A very weak flux intensification at 0016 UT is also associated with an auroral brightening near the spacecraft footpoint.

Polar LBHS images (not shown) indicate a weak localized brightening in the 0025:53 UT image and a strong brightening between images at 0028:20 and 0030:47 UT; these times are consistent with the weaker and stronger AKR onsets cited above. LBHL images at 0029:34 and 0034:28 UT in Plate 5 demonstrate that this event occurred west of spacecraft 095 near 2100 LT which is an earlier local time than usual. The fact that GOES 8 (not shown) at 1930 LT observed sudden increases at 0031 and 0035 UT approaching 20 nT is consistent with the early local time of this onset. Also, the fact that Canadian magnetic observatories at Rankin Inlet, Eskimo Point, and Fort Churchill near 2000 LT (not shown) saw negative bays as large 700 nT following this onset is further testimony to the early local time of this event. The corresponding electrojet moved north with the auroral images during the 20 min after the onset as can be seen in the remaining images. The AKR data indicate another lower-frequency intensification at 0044:25 UT which corresponds to a separate new brightening in the 0044:35 UT image slightly before local midnight. Geotail, still in the tail lobe, sees a preceding increase in B_z and decrease in B at 0042:45 UT and similar, weaker features again follow at IMP 8. Several flow bursts after 0100 UT occur during continuing geomagnetic activity and are difficult to interpret since they are associated with movement in and out of the plasma sheet boundary layer.

This day illustrates lobe field decreases and B_z increases during a relatively large substorm and how they correspond to auroral brightenings, AKR intensifications and geosynchronous dispersionless particle increases when such spacecraft are located in the appropriate local time sector. The lobe field decrease at 16.6 R_E began about a minute before the beginning of the intensification of AKR providing further evidence that substorm phenomena begin in the tail. The lobe field decrease propagated down the tail to IMP 8 with a velocity of about 360 km/s. Dispersionless particle increases at geosynchronous orbit were again delayed by a few minutes relative to other phenomena.

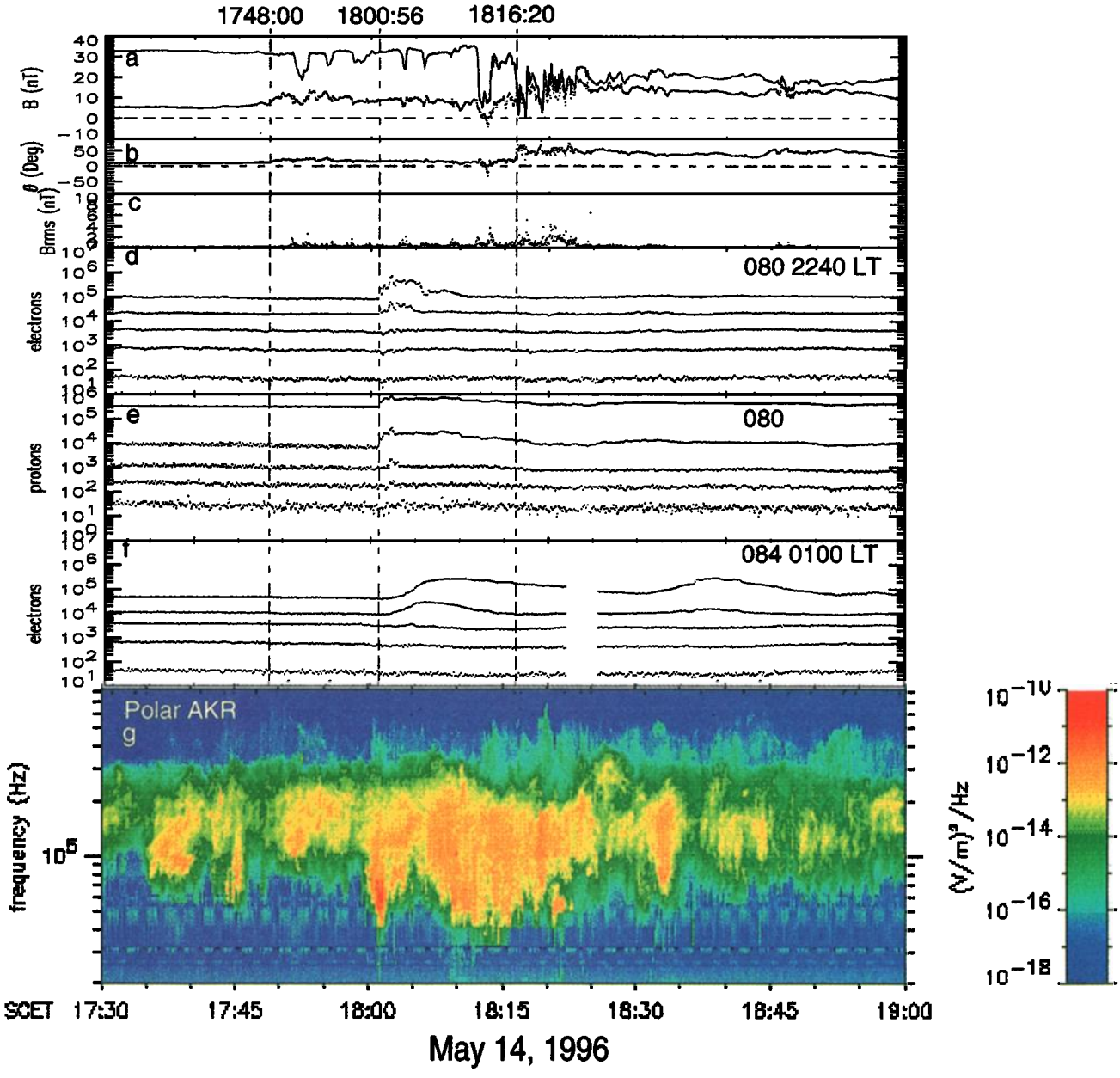

Plate 2. Showing Geotail magnetic field magnitude and B_z (panel a), latitude angle (panel b), magnetic field rms (panel c), and energetic electron fluxes (5 energy channels between 50 keV to 1.1 MeV) from two geosynchronous spacecraft (panels d and f), proton fluxes (5 energy channels between 50–250 keV in panel e), and Polar AKR data (panel g). Geotail data is obtained at too early a local time (1900) to see the effects of the 1800 UT dispersionless onset seen by a geosynchronous spacecraft at 2240 LT. The most intense AKR of the interval precedes the dispersionless onset by 1 or 2 minutes.

3. Flow Burst Characteristics

To further illustrate the characteristics of flow bursts, six such events are displayed in Figure 7. In each row of Figure 7, 20 min of data are shown in each panel centered on the time t=0, which is defined by the increase in B_z and the beginning of disturbed magnetic fields. The first column displaying flow velocities shows that t=0, also corresponds to the beginning of large flow velocities, although it should be noted that in most events the flows start increasing slightly before t=0. as has been noted by *Nagai et al.* [1998] and *Shiokawa et al.* [1998]. Density changes at t=0 are either positive or negative, but these observations may be influenced by the facts that (1) artificially low densities may be obtained if energetic particles above the range of the LEP plasma experiment contribute to the density but are not included or (2) artificially high densities may be obtained if energetic particles penetrate the detector and produce contaminating background counts in the plasma detector [*Fairfield et al.* 1998]. The total field usually increases at t=0 if the spacecraft is very near a weak field region near the center of the current sheet in which case the latitude angle theta is relatively large before the onset (rows 3, 4, and 5). The total field tends not to increase so much at t=0 if the spacecraft is away from the current sheet center in which case the initial theta tends to be small before onset (rows 1 and 2). It should be appreciated, however, that in all cases the initial fields are much lower than the lobe fields at these distances and the spacecraft is immersed in a high-beta plasma well within the

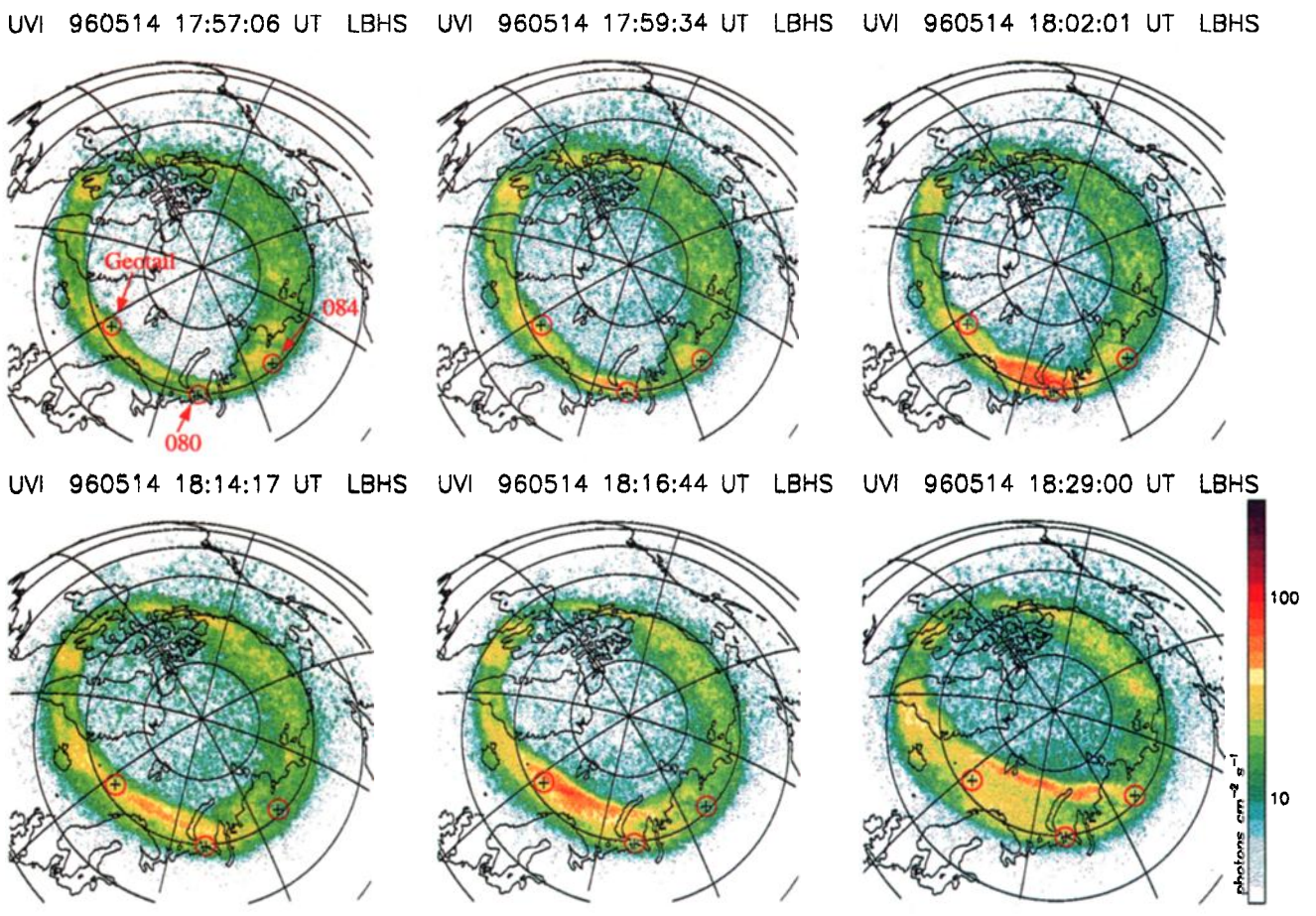

Plate 3. Selected UVI images on May 14, 1996. Spacecraft at locations marked in the 1757:06 image either see or fail to see effects associated with auroral brightenings depending on their proximity to the brightenings (See text).

(probably thinned) plasma sheet .

To further illustrate the nature of flow bursts, Figure 8 shows the B_z component of the high-resolution magnetic field and the corresponding equatorial vector velocity for 10–min intervals around t=0 for the six events of Figure 7. In all events except the third row the velocities are strong and earthward. Missing vectors in the B panel are due to problems associated with very high-velocity flows as discussed by *Fairfield et al.* [1998]. The B_z components are all quite large after t=0, and a large component of the velocity is perpendicular to the magnetic field and is carrying flux earthward. The high-frequency fluctuations are particularly large in the presence of high-velocity flows, suggesting that at least part of these variations are due to spatial structures convecting past the spacecraft. The antisunward flows that frequently follow the several minutes of earthward flows may be part of vortical flows as discussed by *Fairfield et al.* [1998]. (See panel 5 especially.)

To estimate the amount of flux carried earthward past the spacecraft by flow bursts, it is necessary to know the spatial extent of the flow. Knowledge of the Y dimension of the flow is always a problem, but now we have images at the foot of the field line to help estimate this dimension. If we take the bright spots such as in Plate 1 as spanning one hour of local time, we can map that to the equatorial plane using a field model. Using the T87 model and the case of Plate 1 where the spacecraft was located 13 R_E down the tail, we obtain a Y dimension of about 4 R_E. We have selected peak velocities within the flow burst which probably do not prevail over this entire region so an average velocity for a 4 R_E region might be more like 300 km/s. With these assumptions the amount of flux passing the spacecraft vicinity in 1 min would be 60 s × 300 km/s × 10 nT = 113 nTR_e^2 (4.6×10^6W). If this flux were distributed over a 4 R_E region between 6 and 13 R_E it would increase the field by 4 nT, a reasonable number given the uncertainties involved.

4. Summary and Discussion

The comprehensive ISTP data for the events described above help integrate a number of earlier observations and illuminate an emerging picture of energy transport in the magnetic tail. Several examples confirm that flow bursts are characterized by high-velocity flows that can approach 1000 km/s or higher. The flow bursts have durations of the order of a minute, and they tend to occur within intervals of lower flow that are several times as long [*Angelopoulos et al.*, 1992]. They sometimes appear to be intensifications of ongoing vortical flow in the equatorial plane. B_z increases during a flow burst, and highly fluctuating magnetic fields accompany the rapid flows. Flows observed very near the equatorial plane tend to be confined to this plane and hence have a large component perpendicular to the primarily northward magnetic field. Sometimes, however, the transition to a large, persistently northward magnetic field is delayed by a couple of minutes in which case the field-aligned component is initially significant. The above facts confirm that considerable energy and magnetic flux is carried earthward by these bursts [*Angelopoulos*

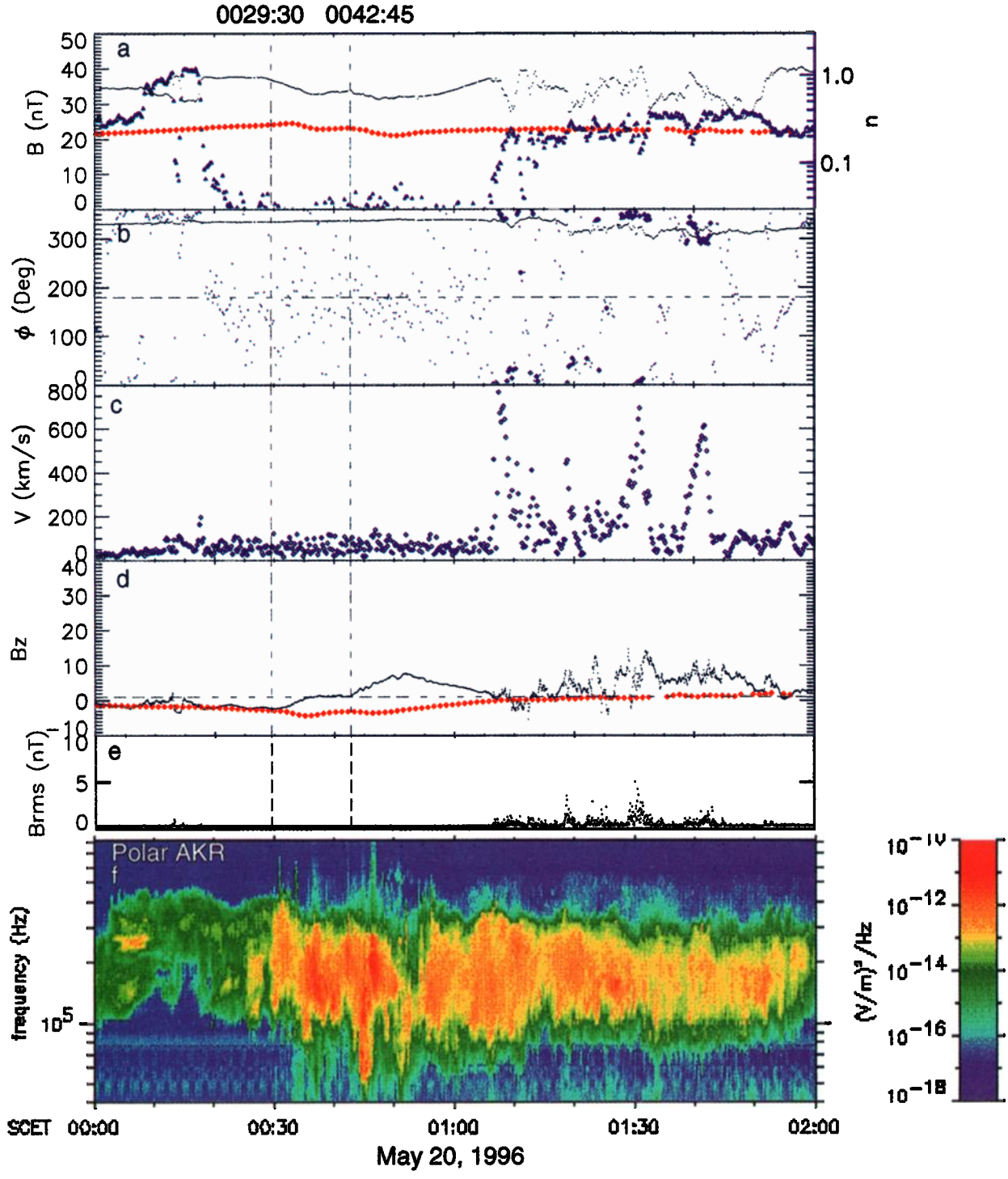

Plate 4. Illustrating Polar AKR data along with Geotail (black) and Imp 8 (red) magnetic field data and Geotail plasma data (blue). Vertical dashed lines indicate two AKR onsets/intensifications that correspond to tail lobe B and B_z changes, with those at Geotail occurring before those at Imp 8 which 17 R_E further down the tail.

et al., 1996; *Fairfield et al.*, 1998]. At greater distances from the plane where measurements are more common, a larger component of the flow is along the primarily B_x-directed magnetic field.

By first selecting flow bursts and then comparing them with other phenomena, we conclude that flow bursts are closely associated with both auroral brightenings, AKR intensifications, ground magnetic disturbances, and geosynchronous particle injections. Were one to select events using only these other phenomena, it would be difficult to make this association since flow bursts are very localized and spacecraft are frequently not at the relevant longitude and in the appropriate equatorial position to observe them.

In the events with images available, auroral brightenings were observed near the longitudes of the footpoint of the spacecraft measuring the flow burst. Additional brightenings away from the footpoint were not associated with observations of flow bursts al-

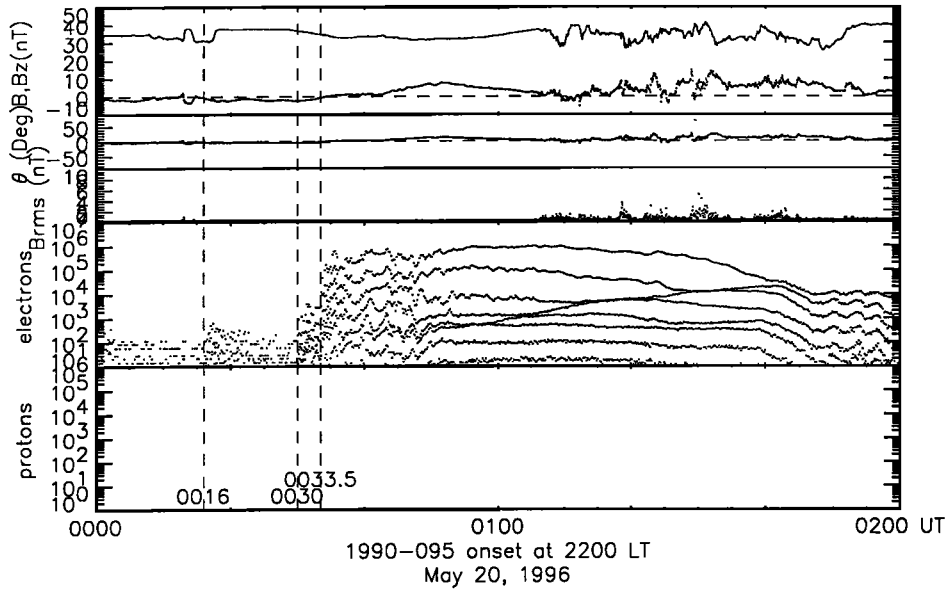

Figure 6. Geotail magnetic field in the tail lobe are shown along with energetic electron fluxes from a Los Alamos geosynchronous spacecraft. The flux increases occur at times corresponding to AKR intensifications.

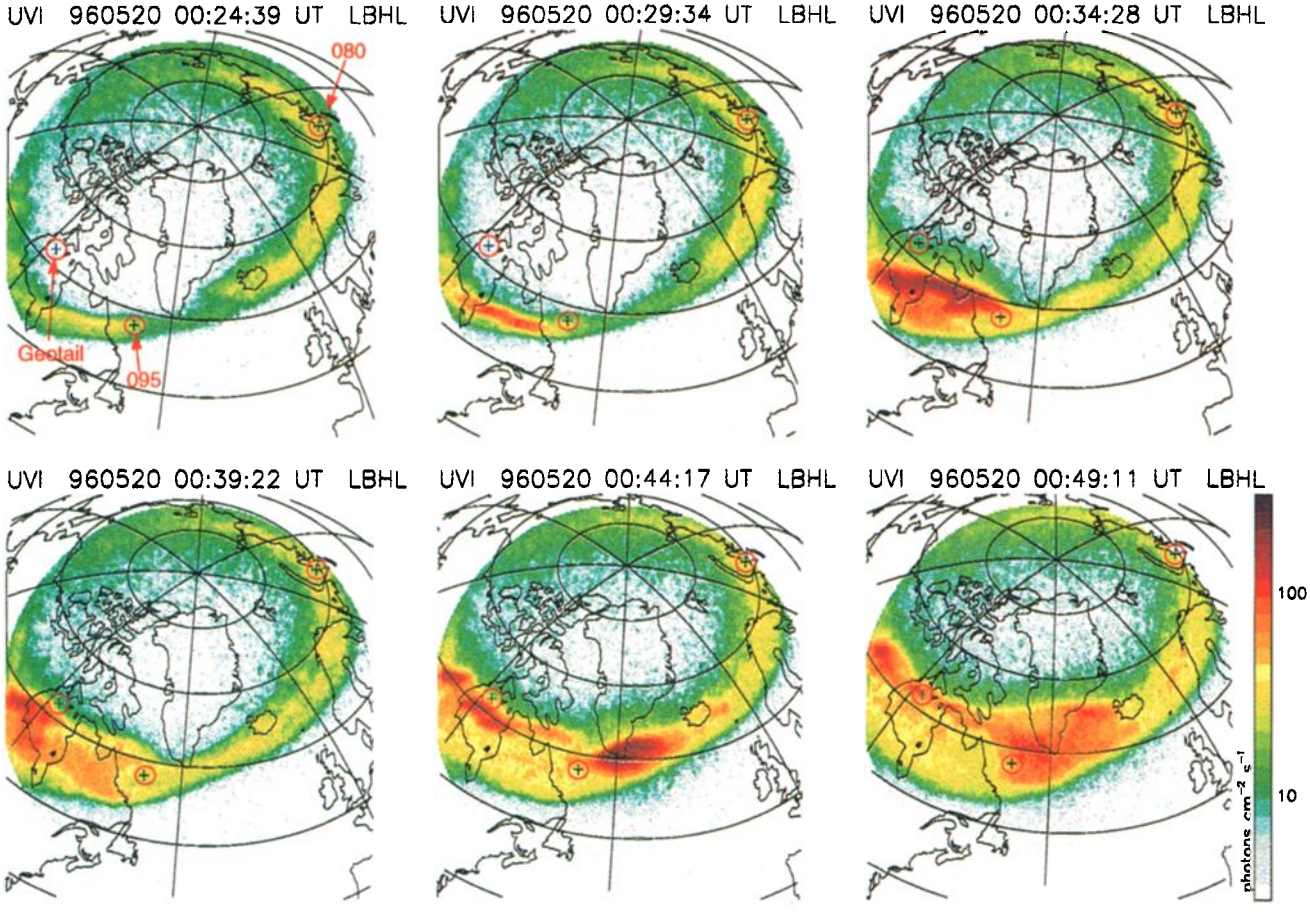

Plate 5. Selected UVI images on May 20, 1996. Auroral brightenings are associated with both the 0029:30 and 0042:45 Geotail tail lobe changes that are themselves associated with AKR intensifications. The earlier onset occurs just west of the geosynchronous spacecraft 095 which detects the injection. The later injection occurred east of this spacecraft which did not detect eastward drifting electrons. Proton data was unavailable.

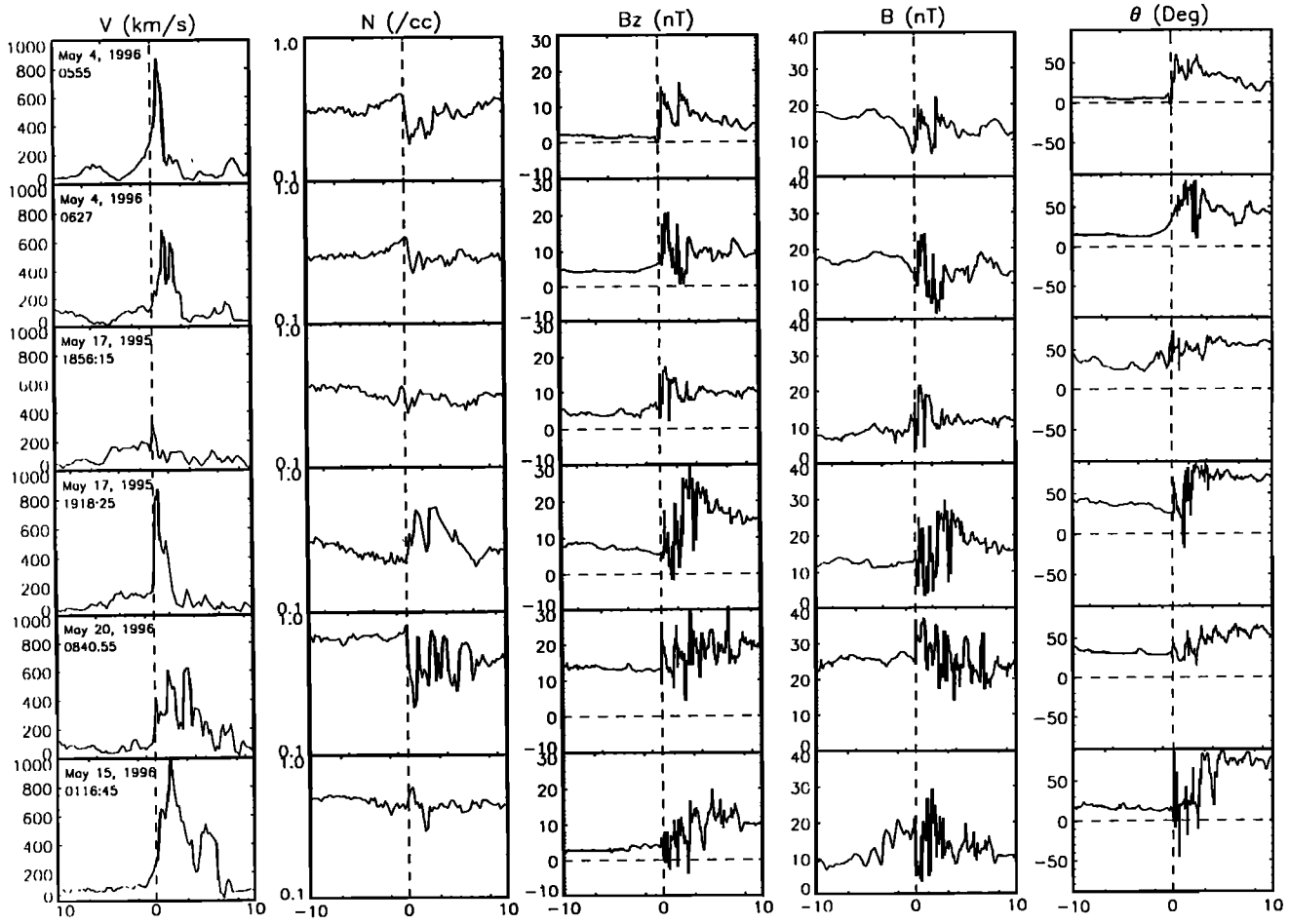

Figure 7. Five different parameters are shown relative to onset times defined by the B_z increase. The onset time could have equally well been determined from the start of high velocity flows.

though magnetic field reconfigurations were sometimes observed, if only on a delayed basis. This latter observation is consistent with the well-known fact that a localized current wedge gradually expands in longitude over the course of a substorm. It should be emphasized that although earthward flow bursts are localized and quickly carry significant magnetic flux earthward, the result of the process is frequently a global reconfiguration of the field as is manifested by a more gradual increase in B_z over a broad region.

Flow–burst–associated brightenings and accompanying phenomena were not always large enough to be labeled substorms which is consistent with the earlier observation that flow bursts can occur during quiet times [e.g., *Angelopoulos et al.*, 1992]. It is also consistent with the suggestion that flow bursts form the smallest fundamental process in substorms but only evolve into a more global magnetospheric substorm under certain unknown conditions [*Sergeev* 1992, *Elphinstone et al.*, 1995b]. Ground magnetic activity also seems to be formed from small discreet events [*Rostoker*, 1991] which may well be the ground manifestation of these same processes.

AKR intensifications usually occurred within a minute of the flow burst, although these intensifications were sometimes weak and/or their onset times uncertain to about a minute. When dispersionless particle increases were measured at geosynchronous orbit, their onset times tended to follow the AKR onsets by 1–3 min. This fact is in agreement with other recent results which indicate that the injection region propagates inward [*Reeves et al.*, 1996; *Fairfield et al.*, 1998; *Shiokawa et al.*, 1998; *Maynard et al.*, 1996]. This observation supports a scenario where the sudden brightening dipolarization events are initiated in the tail with information propagating rapidly along field lines to the high-latitude ionosphere but particle acceleration and transport to geosynchronous orbit taking slightly longer. These points also agree with simulation results of *Birn and Hesse* [1996] where tail reconnection initiates earthward flows, field-aligned currents, and particle acceleration. Our data are consistent with the data of *Shiokawa et al.* [1997; 1998] and their ideas emphasizing the importance of the braking mechanism and shear flows in producing the current wedge in the inner magnetosphere. The data, however, do not preclude the possibility that more subtle effects such as initial slow brightening and magnetosphere/ionosphere information exchange advocated by *Maynard et al.* [1996] occur at an earlier time.

It should be noted that the auroral brightenings associated with our selected flow bursts appear to occur near the poleward boundary of the auroral oval, whereas substorm onsets typically occur nearer the center of the oval, and hence on field lines that close well earthward of any neutral line [e.g., *Lyons et al.*, 1998]. This observation raises the question as to whether we may have

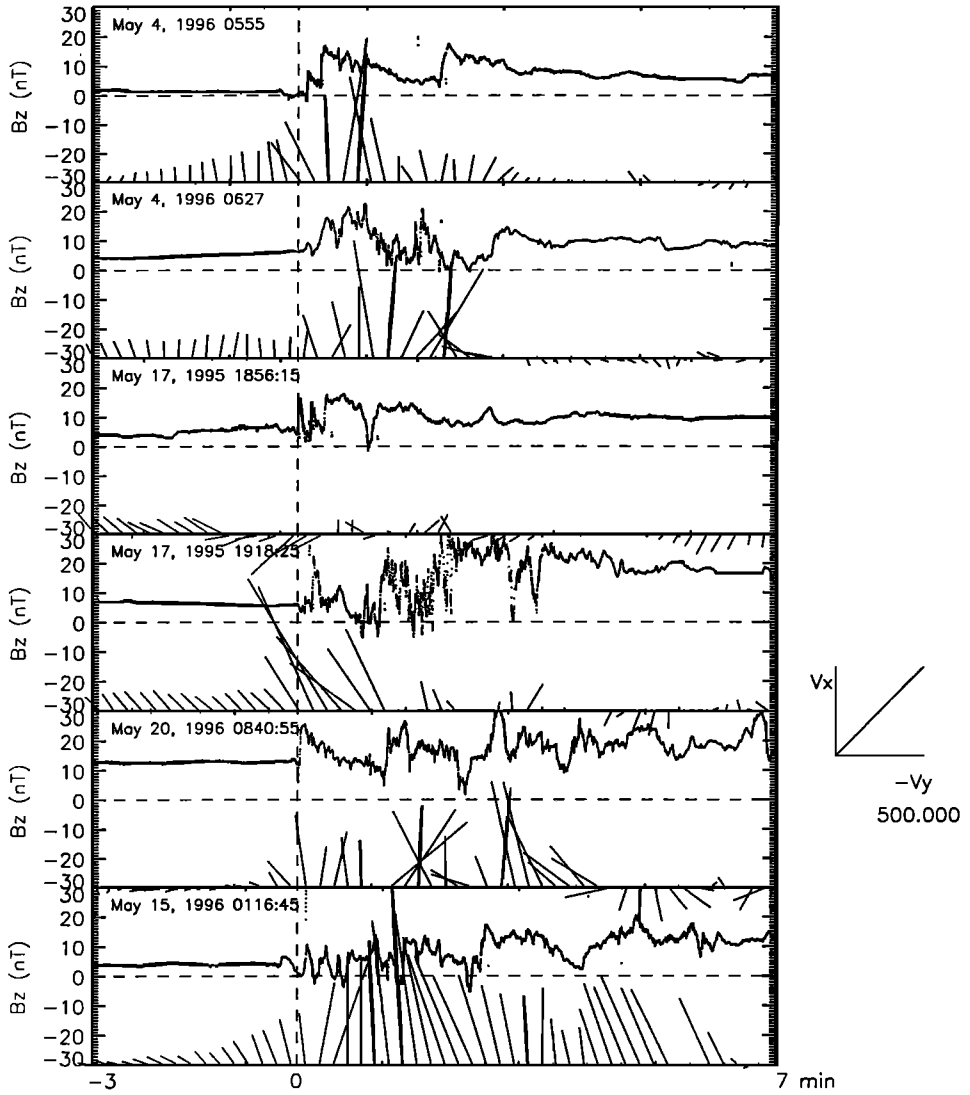

Figure 8. High resolution magnetic field and velocity vectors are shown for six flow bursts. Most events show slow tailward flows after the initial earthward flow bursts, suggesting a connection to vortices.

selected particular types of high-latitude events by first choosing the tail flow bursts. Such boundary and lower-latitude events have been distinguished by *Elphinstone et al.* [1995a]. On the other hand, onset aurora move rapidly poleward [e.g., *Lyons et al.*, 1998], and the time and spacial resolution in our images may not be adequate to make this distinction.

5. Conclusions

Investigation of flow bursts at 10 – 15 R_E in the premidnight equatorial magnetotail demonstrates that such events are closely associated with auroral brightenings, AKR onsets, geosynchronous particle injections, and ground magnetic activity. Timing of the various phenomena supports the view that flow bursts probably precede the sudden changes that characterize related phenomena and hence the events are initiated in the magnetotail beyond 15 R_E. In particular these results support a picture where reconnection near 25 R_E creates earthward convective flow in a spacially limited region near the equatorial plane. (See Figure 9 for a schematic illustration of the events associated with flow bursts.) At velocities of 1000 km/s (9 R_E/min) or higher this plasma rapidly carries energy and magnetic flux to the inner magnetotail where they may initiate processes associated with substorm onset. The large electric fields associated with this process accelerate the particles that cause "dispersionless injections" at geosynchronous orbit [*Birn et al.*, 1997] with time delays typically 1–3 min [see also *Reeves et al.*, 1996]. Reconnection and subsequent acceleration also produce energetic particles that are more field aligned [e.g., *Nagai et al.*, 1998], and it is also possible that these particles quickly reach low altitudes and initiate the auroral acceleration processes at several thousand kilometers altitude that produce the brightened aurora that denote substorm onsets and pseudo-onsets. The close association with AKR and auroral breakups poses the question of how particles accelerated in the tail effect the auroral acceleration process and the associated production of AKR at a few thousand kilometer altitude.

Although this work favors the near-Earth neutral line as the origin of substorms onsets, it should be noted that the auroral brightenings associated with our selected flow bursts tend to occur near the poleward boundary of the auroral oval. Although it

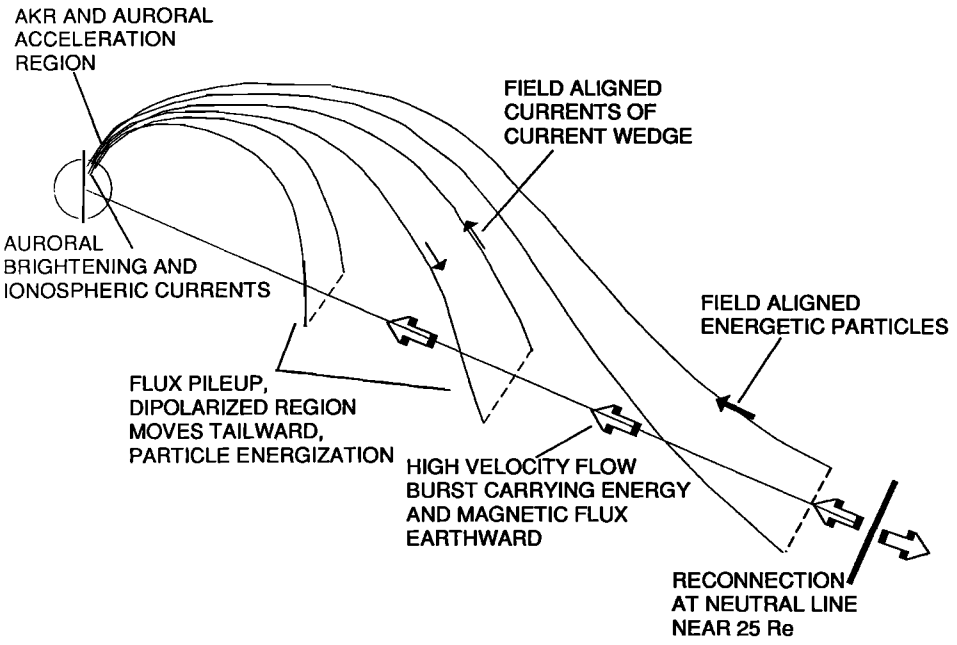

Figure 9. A schematic illustration of events associated with flow bursts in the magnetotail.

seems likely that rapid earthward flows from the neutral line can quickly initiate substorms on lower-latitude field lines, it is possible that we may have selected particular class of high-latitude onset events; other lower-latitude substorm onsets on field lines that close well earthward of a neutral line might originate in a different manner.

Acknowledgments. Discussions with M. Hesse are gratefully acknowledged. The CANOPUS array was constructed and is operated and maintained by the Canadian Space Agency. Additional magnetograms used in this work were provided by the Geological Survey of Canada. G.D.R. acknowledges the support of the DoE Office of Basic Energy Science.

The Editor thanks W. J. Burke and G. T. Blanchard for their assistance in evaluating this paper.

References

Angelopoulos, V., W. Baumjohann, C. F. Kennel, F. V. Coroniti, M. G. Kivelson, R. Pellat, R. J. Walker, H. Luhr, and G. Paschmann, Bursty bulk flows in the inner central plasma sheet, *J. Geophys. Res.*, *97*, 4027, 1992.

Angelopoulos, V., et al., Multipoint analysis of a bursty bulk flow event on April 11, 1985, *J. Geophys. Res.*, *101*, 4967, 1996, (Correction, J. Geophys. Res., 102, 211, 1997).

Birn, J., and M. Hesse, Details of current disruption and diversion in simulations of magnetotail dynamics, *J. Geophys. Res.*, *101*, 15,345, 1996.

Birn, J., M. F. Thomsen, J. E. Borovsky, G. D. Reeves, D. J. McComas, and R. D. Belian, Substorm ion injections: Geosynchronous observations and test particle orbits in three-dimensional dynamic MHD fields, *J. Geophys. Res.*, *102*, 2325, 1997.

Elphinstone, R. D., et al., The double oval UV auroral distribution, 1. Implications for the mapping of auroral arcs, *J. Geophys. Res.*, *100*, 12,075, 1995a.

Elphinstone, R. D., et al., Observations in the vicinity of substorm onset: Implications for the substorm process, *J. Geophys. Res.*, *100*, 7937, 1995b.

Fairfield, D. H., A statistical determination of the shape and position of the geomagnetic neutral sheet, *J. Geophys. Res.*, *85*, 775, 1980.

Fairfield, D. H., et al., Geotail observations of substorm onset in the inner magnetotail, *J. Geophys. Res.*, *103*, 103, 1998.

Gurnett, D. A., The Earth as a radio source: Terrestrial kilometric radiation, *J. Geophys. Res.*, *79*, 4227, 1974.

Kaiser, M. L., and J. K. Alexander, Relationship between auroral substorms and the occurrence of terrestrial kilometric radiation, *J. Geophys. Res.*, *82*, 5283, 1977.

Kaneda, E., and T. Yamamoto, Auroral substorms observed by UV-imager on Akebono, in *Magnetospheric Substorms, Geophys. Monogr. Ser.*, edited by J. R. Kan, T. A. Potemra, S. Kokubun, and T. Iijima, vol. 64, p. 235, AGU, Washington DC, 1991.

Lewis, R. V., M. P. Freeman, A. S. Rodger, M. Watanabe, and R. A. Greenwald, The behavior of the electric field within the substorm current wedge, *J. Geophys. Res.*, *103*, 179, 1998.

Lopez, R. E., A. T. Y. Lui, D. G. Sibeck, K. Takahashi, R. W. McEntire, L. J. Zanetti, and S. M. Krimigis, On the relationship between the energetic particle flux morphology and the change in the magnetic field magnitude during substorms, *J. Geophys. Res.*, *94*, 17,105, 1989.

Lui, A. T. Y., Current disruption in the Earth's magnetosphere: Observations and models, *J. Geophys. Res.*, *101*, 13,067, 1996.

Lyons, L. R., G. T. Blanchard, J. C. Samson, J. M. Ruohoniemi, R. A. Greenwald, G. D. Reeves, and J. D. Scudder, Near Earth plasma sheet penetration and geomagnetic disturbances, in *Magnetospheric Substorms, Geophysical. Monograph. Series.*, AGU, Washington D.C. in press, 1998.

Maynard, N. C., W. J. Burke, E. M. Basinska, G. M. Erickson, W. J. Hughes, H. J. Singer, A. G. Yahnin, D. A. Hardy, and F. S. Mozer, Dynamics of the inner magnetosphere near times of substorm onsets, *J. Geophys. Res.*, *101*, 7705, 1996.

Murphree, J. S., R. D. Elphinstone, L. L. Cogger, and D. Hearn, Viking optical substorm signatures, in *Magnetospheric Substorms, Geophys. Monogr. Ser.*, edited by J. R. Kan, T. A.

Potemra, S. Kokubun, and T. Iijima, vol. 64, p. 241, AGU, Washington DC, 1991.

Nagai, T., et al., Structure and dynamics of magnetic reconnection for substorm onsets with Geotail observations, *J. Geophys. Res.*, *103*, 4419, 1998.

Petrukovich, A. A., et al., Two spacecraft observations of a reconnection pulse during an auroral breakup, *J. Geophys. Res.*, *103*, 47, 1998.

Pulkkinen, T. I., et al., Two substorm intensifications compared: Onset, expansion and global consequences, *J. Geophys. Res.*, *103*, 15, 1998.

Reeves, G. D., M. G. Henderson, P. S. McLachlan, R. D. Belian, R. H. W. Friedel, and A. Korth, Radial propagation of substorm injections, in *Third International Conference on Substorms, Eur. Space Agency Spec. Publ., SP-389*, p. 579, 1996.

Rostoker, G., Some observational constraints for substorm models, in *Magnetospheric Substorms, Geophys. Monogr. Ser.*, edited by J. R. Kan, T. A. Potemra, S. Kokubun, and T. Iijima, vol. 64, p. 61, AGU, Washington DC, 1991.

Rostoker, G., On the place of the pseudo-breakup in a magnetospheric substorm, *Geophys. Res. Lett.*, *25*, 217, 1998.

Sergeev, V. A., Tail-aurora direct relationship, in *Substorms 1, Eur. Space Agency Spec. Publ., 335*, p. 277, 1992.

Sergeev, V. A., Magnetic reconnection: A cause or a consequence?, in *Third International Conference on Substorms, Eur. Space Agency Spec. Publ., SP-389*, p. 479, 1996.

Sergeev, V. A., T. I. Pulkkinen, and R. J. Pellinen, Coupled-mode scenario for the magnetospheric dynamics, *J. Geophys. Res.*, *101*, 13,047, 1996.

Shiokawa, K., et al., High speed ion flow, substorm current wedge, and multiple Pi 2 pulsations, *J. Geophys. Res.*, *103*, 4491, 1998.

Shiokawa, K., W. Baumjohann, and G. Haerendel, Braking of high-speed flows in the near-Earth tail, *Geophys. Res. Lett.*, *24*, 1179, 1997.

Torr, M. R., et al., A far ultraviolet imager for the international solar-terrestrial physics mission, *Space Sci. Rev.*, *71*, 329, 1995.

Tsyganenko, N., Effects of the solar wind conditions on the global magnetospheric configuration as deduced from data-based field models, in *Third International Conference on Substorms, Eur. Space Agency Spec. Publ., SP-389*, p. 181, 1996.

Tsyganenko, N. A., Global quantitative models of the geomagnetic field in the cislunar magnetosphere for different disturbance levels, *Planet. Space Sci.*, *35*, 1347, 1987.

Tsyganenko, N. A., Modeling the Earth's magnetospheric magnetic field confined within a realistic magnetopause, *J. Geophys. Res.*, *100*, 5599, 1995.

Voots, G. R., D. A. Gurnett, and S. I. Akasofu, Auroral kilometric radiation as an indicatior of auroral magnetic disturbances, *J. Geophys. Res.*, *82*, 2259, 1977.

Williams, P. J. S., R. V. Lewis, T. S. Virdi, M. Lester, and E. Nielsen, Plasma flow bursts in the aororal electrojets, *Ann. Geophys.*, *10*, 835, 1992.

Yahnin, A., V. A. Sergeev, B. B. Gvozdevsky, and S. Vennerstrom, Magnetospheric source region of discrete auroras inferred from their relationship with isotropy boundaries of energetic particles, *Ann. Geophys.*, *15*, 943, 1997.

M. Brittnacher and G. K. Parks, Geophysics Program, University of Washington, Seattle, WA 98195. (e-mail: britt@geophys.washington.edu; parks@geophys.washington.edu)

D. H. Fairfield, Code 695, NASA Goddard Space Flight Center, Greenbelt, MD. (e-mail: u2dhf@lepdhf.gsfc.nasa.gov)

D. A. Gurnett, Department of Physics and Astronomy, University of Iowa, Iowa City, IA 52242. (e-mail: gurnett@space.physics.uiowa.edu)

S. Kokubun, STELAB, Nagoya University, Toyokawa 442, Japan. (e-mail: kokubun@stelab.nagoya-u.ac.jp

H. Matsumoto and K. Hashimoto, Radio Atmospheric Science Center, Kyoto University, Uji, Kyoto 611, Japan (e-mail: matsumot@kurasc.kyoto-u.ac.jp; ko:::@kurasc.kyoto-u.ac.jp)

T. Mukai, ISAS, Sagamihara 229, Japan. (e-mail: mukai@fujitubo.gtl.isas.ac.jp)

G. D. Reeves, Mail Stop D-436, Los Alamos National Laboratory, Los Alamos, NM 87545. (e-mail: reeves@lanl.gov)

(Received April 30, 1998: revised July 10, 1998:
accepted July 30, 1998.)